

# Creating Advanced Dual-Channel Paired-Waves Surface Plasmon Resonance (PWSPR) Biosensor for Detection of MiR-21 MicroRNA

Ying-Chang Li<sup>1\*</sup>, Li-Chen Su<sup>2</sup>, Chiu-Chian Chiou<sup>3</sup>, Chien Chou<sup>4</sup>

## ABSTRACT

In biomedical research, microRNAs (miRNAs) are key for gene regulation and early disease detection. Our study unveils an advanced optical device, a dual-channels paired-waves surface plasmon resonance (PWSPR) biosensor, for direct, label-free miRNA detection, focusing on microRNA-21-5p (miR-21). This miRNA is vital in regulating cell death, growth, and movement. Remarkably, our device detects the 15-mer central segment of miR-21 with high sensitivity, achieving a detection limit of 50 picomolar (pM), far exceeding traditional methods. Additionally, by analyzing various concentrations of miR-21, our system precisely determines the affinity constant ( $K_A$ ) of  $3.7 \times 10^8 M^{-1}$  between the capture probe and miR-21, offering insights into the binding efficiency. This breakthrough indicates the dual-channel PWSPR platform's potential to transform miRNA detection and analysis, such as miR-21, enhancing biomedical research's efficiency and sensitivity. It opens new avenues for early disease diagnosis and a deeper understanding of gene regulation mechanisms.

**Keywords:** microRNA (miRNA), point mutation, surface plasmon resonance (SPR) biosensor, early disease diagnosis

## I. INTRODUCTION

MicroRNA (miRNA) represents a class of small, non-coding RNA molecules that play a pivotal role in the regulation of gene expression at the post-transcriptional level, holding significant implications for health, disease, and developmental processes [1-2]. Owing to their stability in bodily fluids, miRNAs are considered promising

candidates for disease biomarkers. Among them, miR-21-5p (miR-21) stands out as one of the most abundantly expressed and extensively studied miRNAs [3]. Functionally, miR-21 exhibits a broad spectrum of activities. In both oncological and non-oncological diseases, the downregulation of miR-21 has been associated with increased cell mortality [4-6]. Conversely, in cardiovascular diseases, miR-21 contributes to fibrosis and cardiac hypertrophy [7-9]. Thus, in fluid-based miRNA research, miR-21 is frequently identified as a biomarker for conditions such as cancer and heart disease, and it is also being explored for its diagnostic potential in neurodegenerative diseases.

In the rapidly evolving realm of biotechnology, the research and development of biosensors have emerged as a field brimming with potential and fervor. Biosensors are devices that utilize bio-recognition elements with biochemical specificity, such as enzymes, lectins, antibodies, receptors, and nucleic acids, to detect target analytes [10-11]. These recognition elements respond to the analytes and generate biological signals. These signals are then converted by a transducer into a recognizable form, such as electrical, electrochemical, optical, thermal, or piezoelectric signals [12]. If the converted signal is too weak, an amplifier is required to produce a measurable signal proportional to the concentration of the target analyte. Biosensors find extensive applications in environmental monitoring [13], disease diagnosis [14], food safety testing [15], and drug development [16-17]. With advancements in bioengineering, particularly in molecular biology and nanotechnology, the sensitivity and specificity of biosensors have been significantly enhanced. Moreover, the integration of modern optical measurement techniques, such as fluorescence labeling [18-19], Surface Plasmon Resonance (SPR) [20-22], and Optical Waveguide Lightmode Spectroscopy (OWLS) [23-24], has substantially augmented the detection capabilities of biosensors, enabling them to identify target analytes with greater precision at lower concentrations and in shorter timeframes.

Regarding the classification of biomedical sensor sensing modes, there are two types: Label-based and Label-free. Label detection primarily utilizes 'tags' or 'labels' to identify specific analytes in complex testing environments. Labeling technology often involves fluorescent, chemiluminescent, and nanoparticle technologies for bond labeling followed by detection [25-27]. However, the labeling process is intricate and

\*Corresponding Author: Ying-Chang Li (E-mail: YCLI@ncut.edu.tw).

<sup>1</sup>Graduate Institute, Prospective Technology of Electrical Engineering and Computer Science, National Chin-Yi No.57, Sec. 2, Zhongshan Rd., Taiping Dist., Taichung 411030, Taiwan

<sup>2</sup>The General Education Center, Ming Chi University of Technology, 84 Gungjuan Rd., Taishan Dist., New Taipei City 243303, Taiwan

<sup>3</sup>Department of Medical Biotechnology and Laboratory Science, Chang Gung University, No.259, Wenhua 1st Rd., Guishan Dist., Taoyuan City 33302, Taiwan

<sup>4</sup>Graduate Institute of Electro-Optical Engineering, Chang Gung University, No.259, Wenhua 1st Rd., Guishan Dist., Taoyuan City 33302, Taiwan

time-consuming, and the use of small molecule tags in labeling also increases the measurement cost. Non-label detection employs physical characteristics such as oscillation frequency, refractive index, or charge to detect the presence or characteristics of molecules [28-29]. Its advantage lies in its ability to perform real-time monitoring, observing changes in molecules over time or the rate of intermolecular reactions. Label-free detection uses native proteins or ligands, thereby providing more direct information during measurement.

In the past thirty years, surface plasmon resonance (SPR) technology has become a recognized optical method in the field of optical biomedicine [30-32]. Surface Plasmons (SPs) are electromagnetic waves tightly bound at the interface between a metal and a dielectric. These waves result from the resonance phenomenon created by the collective oscillation of free electrons in the metal interacting with light. When light waves strike the metal surface, they excite these free electrons, leading to the formation of surface waves that propagate along the metal surface, known as Surface Plasmons. In the medical field, SPR biosensors provide non-invasive, instantaneous, and highly sensitive analytical methods, applicable for the diagnosis of diseases such as cancer, cardiovascular disease, and the early detection and monitoring of infectious diseases [33-35]. Using SPR-based biosensors, medical staff can instantly monitor changes in biomarkers, enabling them to conduct accurate diagnoses and treatments based on these changes.

This article presents the establishment of a dual-channel system on a gold film surface, integrated within a PSPW-based platform. Utilizing these dual technologies effectively attenuates noise fluctuations originating from the optical path and the peristaltic pump. Additionally, this investigation harnesses DNA probes for the sensitive detection of oligonucleotides, specifically employing DNA/miRNA dynamics. Single-stranded DNA (ssDNA) probes, immobilized on a gold chip, are utilized for the detection of the complementary miR-21 miRNA. Employing this platform enables the detection of ultra-low concentrations of miR-21, obviating the need for labeling or subsequent labeling steps.

## II. BACKGROUND AND MOTIVATION

A bespoke dual-channel PWSPR apparatus was meticulously configured for the detection of DNA/miRNA hybridization. Demonstrated in Figure A, a Zeeman He-Ne laser apparatus emits a duo of orthogonally linearly polarized waves, distinguished by a specific beat frequency. Through the precision adjustment of a half-wave plate ( $\lambda/2$ ), the laser's linear polarizations are ingeniously rotated by 45 degrees. This manipulation facilitates their subsequent passage through a polarized beam splitter, culminating in the bifurcation into signal and reference beams. Specifically, the signal beam is composed of a pair of p waves, denoted as  $(P_1 + P_2)_{sig}$ , while the reference beam comprises a duo of s waves, represented as  $(S_1 + S_2)_{ref}$ . Notably, both  $(P_1 + P_2)_{sig}$  and  $(S_1 + S_2)_{ref}$  exhibit common-path propagation

within the experimental setup, a strategic design choice. This arrangement ingeniously mitigates common-phase noise attributed to environmental perturbations, such as fluctuations in temperature, through the mechanism of optical heterodyne interference [22].

The PSPWB platform stands out for its exceptional detection sensitivity and ease of use, thanks to several key features. Firstly, it reduces noise through heterodyne interference and synchronized detection, enhancing clarity. Secondly, signal fluctuations are minimized by normalizing detected signals using a demodulated amplitude ratio algorithm for the signal and reference beams. Lastly, PSPWB's amplitude-sensitive detection offers a broader dynamic range compared to the intensity detection found in traditional SPR biosensors, making it a more versatile and reliable choice for biosensing applications. The aforementioned optical system had been successfully established, and its efficacy along with related research findings had been published in a high-quality journal [22, 36].

To enhance the system's sensitivity and reliability, improvements have been made to the microchannel structure. This is crucial as the input device for the flow system is a peristaltic pump, which, when generating peristaltic flow (stress fluid), introduces subtle disturbances to the sidewalls of rectangular microfluidic channels (specifically referring to the sensing chamber, especially the sensing area). The causes of these disturbances include variations in flow velocity, pressure fluctuations, and fluidic diffusion effects across corners. To address these issues, a dual-channel system was established, featuring two identical microchannels operated by the same peristaltic pump. This design ensures that the peristaltic flow generated within the microchannels has similar sources of disturbance. During experiments, one set serves as the experimental channel, while the other functions as the reference channel. The reference channel simultaneously injects the same buffer solution, ensuring that the liquid disturbances created by the peristaltic pump occur concurrently in both the experimental and reference channels. Utilizing a signal subtraction technique significantly reduces the noise generated by fluid disturbances in the microchannels [36].

## III. SYSTEM SETUP

The schematic delineates the dual-channels PWSPR system, including optical setup designed for SPR sensing, incorporating a peristaltic pump for fluid manipulation within the system as shown in Fig. 1. Central to the apparatus is a Zeeman Helium-Neon (HeNe) Laser (ZL), which serves as the coherent light source emitting linearly polarized light. This light is subsequently modulated by a half-wave plate ( $\lambda/2$ ) to adjust its polarization state before being split by a polarized beam splitter.

The PBS functions to produce two orthogonally polarized light waves,  $P_1+P_2$  and  $S_1+S_2$ , which are directed towards a lateral displacement beam splitter (LDB). The

LDB finely adjusts the path of the polarized light beams, ensuring precise interaction with the SPR device's sensor surface, within a Polydimethylsiloxane (PDMS) chamber.

The reflected light beams, now carrying the SPR signal, are redirected by mirrors (M) to their respective detectors (D), capturing the resonance condition induced by the surface-bound analyte. The detectors' output is then processed by lock-in amplifiers (LIA) to enhance the signal-to-noise ratio, providing highly sensitive measurement data which can be correlated to the refractive index changes near the sensor surface, indicative of molecular interactions.

This PWSPR apparatus is coupled with a microfluidic device, featuring a peristaltic pump, tiny tubes for fluid channels, and a custom-fabricated PDMS chamber. This microfluidic device ensures a continuous and controlled flow of the analyte solution through the PDMS chamber. This fluidic control is critical in maintaining consistent analyte delivery and effective washing phases during the assay, contributing to the reproducibility and reliability of the sensor's readings. The entire process is governed by a computer, which synchronizes the data acquisition from two Lock-in amplifiers. Such a system is adept at real-time monitoring of biomolecular interactions, making it an invaluable tool in detecting DNA/RNA hybridization.

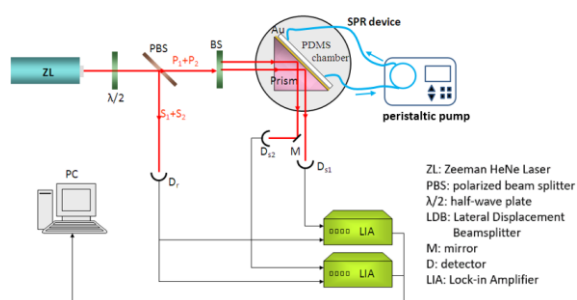


**Figure 1. Schematic of dual-channel paired waves surface plasmon resonance biosensor configuration for detecting DNA/RNA hybridization.**

#### IV. EXPERIMENTAL PROCEDURES

**Materials.** The materials used in this study were sourced from a variety of reputable suppliers to ensure quality and consistency. The oligonucleotide components, specifically synthesized single-strand oligonucleotides purified to OPC-grade, were procured from Purigo, based in Taipei, Taiwan. The ssDNA capture probe targeting miR-21 was engineered to feature complementarity, as delineated in Reference [37]. The specific sequence orientations of the ssDNA capture probe and the miR-21, ranging from the 5' to 3' end, are denoted as SH-C<sub>6</sub>H<sub>12</sub>-AAA AAA AAT CAA CAT CAG TCT GAT AAG CTA (Sequences underlined indicate the parts that bind with the miRNA sequence) and UAG CUU AUC AGA CUG AUG UUG, respectively. This strategic design ensures targeted hybridization, facilitating the precise

detection and quantification of miR-21 within complex biological samples. Phosphate buffered saline (PBS) and 6-Mercapto-1-hexanol (MCH) were purchased from Sigma-Aldrich, St. Louis, MO. 2-Propanol was acquired from J.T. Baker in Phillipsburg, NJ, USA, while absolute ethanol and acetone were sourced from Mallinckrodt Baker in Paris, Kentucky, USA.

The oligonucleotides in question were methodically synthesized into a 100 mM primary stock solution using PBS and subsequently sequestered at -20°C to maintain molecular integrity. To accommodate diverse experimental requirements, working solutions at specified concentrations were meticulously derived by diluting the aforementioned stock with PBS. The detection assays were uniformly conducted at a stringent ambient temperature of 25°C. The detection milieu was a PBS-based buffer, meticulously composed of 10 mM sodium phosphate at a physiological pH of 7.4, and 150 mM NaCl to ensure an exceptionally pure medium conducive to the precise biochemical interactions under scrutiny. All aqueous solutions and the rinsing protocol employed Millipore-filtered water, with a resistivity exceeding 18 Ω cm<sup>-1</sup>, to ensure the utmost purity and reproducibility of results. The formulation of 70% ethanol solution entails the precise dilution of absolute ethanol with de-ionized water (DI H<sub>2</sub>O) to achieve the desired concentration.

**Substrate Preparation.** The SPR sensor chips were fabricated by depositing a 2nm chromium adhesion layer and a 45nm gold film by electron beam evaporation at 10-4 torr or lower. After deposition, the chips underwent a cleaning protocol involving sequential rinses with acetone, 2-propanol, and deionized water, culminating in drying under a stream of nitrogen gas to prepare the surface for biomolecular functionalization.

**Immobilization of ssDNA probe.** In the field of surface-based DNA sensing technologies, the success of hybridization events involving immobilized DNA probes heavily depends on the spatial arrangement of the probes and the distance between them. Our study tackled these critical factors by investigating an immobilization strategy that involves attaching DNA probes, each tagged with a terminal thiol group (DNA-SH), onto a gold surface, as illustrated in figure 2. This approach laid out the foundational methodology for immobilizing the ssDNA probes, ensuring that their positioning and spacing were optimal for effective hybridization [22]. Our experimental framework delineated the principal immobilization methodology as follows:

1. The sensor surface was immersed in a piranha solution with a volumetric ratio of 1:1 sulfuric acid to hydrogen peroxide (H<sub>2</sub>SO<sub>4</sub>: H<sub>2</sub>O<sub>2</sub>) for 2 minutes and then followed by an exhaustive rinse using DI H<sub>2</sub>O. After washing, the sensor was bathed in 70% ethanol for 3 minutes and then rinsed with DI H<sub>2</sub>O. Finally, the sensor surface was air dried at 25 °C for 30 minutes, resulting in a pristine surface suitable for high-sensitivity applications.

2. The SPR device necessitates the assembly of the glass side of the gold-coated BK7 chip onto the rear facet of the prism. At this junction, it is imperative to introduce refractive index matching oil to eradicate any air bubbles that could compromise the contact interface. Following the assemblage, the SPR device is seamlessly integrated into the optical system and interfaced with the microfluidic apparatus.

3. Upon completion of the installation, PBS solution is propelled through the microfluidic channels, inundating the sensing surface to establish a baseline signal within an aqueous milieu. Subsequent signal analyses post-reaction are conducted strictly within the PBS environment to uphold the uniformity of the measurement conditions.

4. The formation of the Self-Assembled Monolayer (SAM) is then initiated. The SAM formation was executed by immersing the cleaned sensor surface in a dilute thiolated oligonucleotide probe solution (40 µg/ml in PBS) for 24 hours, ensuring a stable and functionalized sensing interface.

5. After probe attachment, the surface was passivated by immersion in a 5 mM MCH solution (in PBS) for 24 hours or longer at room temperature, followed by a final PBS rinse to ensure the removal of non-specifically bound molecules.

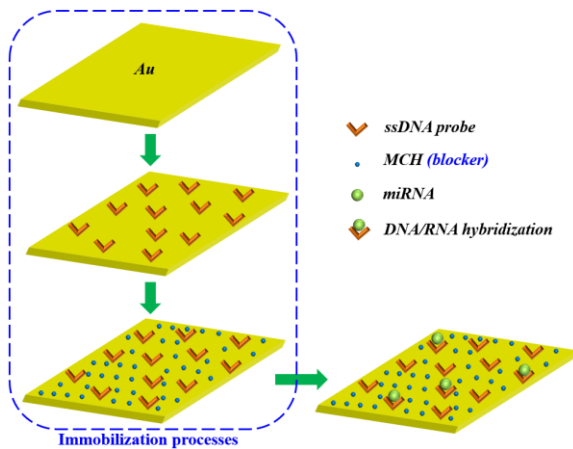


**Figure 2. Schematic of the immobilization of SAM and DNA/RNA hybridization.**

**DNA/RNA Hybridization.** In this study, the miR-21 target was first diluted to a precise concentration of 1 mM in PBS, then further adjusted to a range of concentrations from 1 to 500 nM through serial dilution. During the experimental process, the diluted miR-21 solutions were introduced into the reaction chamber using a peristaltic pump at a rate of 20 µL/min for 30 minutes at room temperature to ensure optimal interaction. Following this hybridization period, the sensor chip underwent a wash with PBS at 200 µL/min for 5 minutes to remove any unbound oligonucleotides, thus preparing it for accurate

detection of hybridization events. The hybridization signal was quantified by analyzing PBS records over a 100-second interval, capturing the mean signal and its variability with precision. The response was quantified utilizing the following formula [22]:

$$R = M_F - M_I \pm 3 \times \sqrt{(S.D._F)^2 + (S.D._I)^2} \quad (1)$$

Where the term  $R$  stands for the signal response.  $M_F$  and  $M_I$  represent the average values observed during a 100-second interval for the final and initial states, respectively. Similarly,  $S.D._F$  and  $S.D._I$  denote the standard deviations for these states within the same timeframe. Given the risk of RNA degradation by ribonucleases (RNases) present in the environment, it's crucial to clean the sample preparation areas with a 10% bleach solution to prevent RNase contamination. Additionally, to avoid the homodimerization of miRNA-21\_tar and ssDNA-21\_Caption, both samples were heated to 70°C for 10 minutes and then rapidly cooled to room temperature before being introduced into the reaction chamber, ensuring the integrity and specificity of the hybridization process.

**Langmuir Isotherm.** The simple Langmuir Isotherm provides a foundational framework for understanding the adsorption of molecules on a surface, essential for interpreting DNA/RNA hybridization experiments [38-39]. It assumes a uniform surface with a finite number of identical sites, where each site can hold only one molecule, and the process is reversible. This model is particularly useful in our context as it helps predict the behavior of nucleic acid strands binding to a solid surface under equilibrium conditions. By applying the Langmuir Isotherm, we can quantify the relationship between the concentration of nucleic acids in solution and their adsorption on the biosensor surface, offering insights into the efficiency and specificity of the hybridization process. The Langmuir isotherm can be mathematically represented as:

$$\Theta = \frac{K_A c_0}{1 + K_A c_0} \quad (2)$$

Where  $\Theta$  is the fractional coverage defined as  $\Gamma/\Gamma_m$  ( $\Gamma_m$  is the miRNA maximum coverage),  $c_0$  is the bulk miRNA target concentration, and  $K_A$  can be deduced by using eq (2) for fitting.

## V. RESULTS AND DISCUSSION

Figure 3 showcases the complete immobilization process involving the ssDNA probe capture and the use of MCH as a blocker. During this experiment, the introduction of the thiolated ssDNA probe into the chamber led to an immediate bond formation between the thiol groups' sulfur atoms and the gold surface, resulting in a sharp increase in the amplitude ratio response in this measurement. Following this, a PBS wash was applied to remove any probes that

hadn't bound, which slightly reduced the signal. This step effectively raised the amplitude ratio response by 0.71 arbitrary units (a.u.) as shown in Fig. 3. Subsequently, injecting the MCH solution into the sensing chip aimed to occupy the spaces between the already immobilized ssDNA molecules, leading to a denser and more uniform layer. Additionally, the hydroxyl group present in MCH played a significant role in creating a hydrophilic surface, further reducing the likelihood of non-specific interactions and enhancing the overall specificity of the immobilization process.

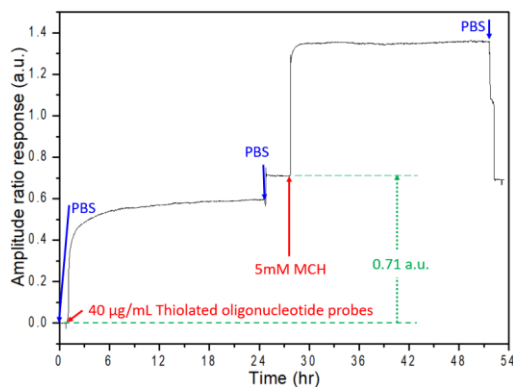


**Figure 3. Magnitude response of probe immobilization by using thiolated single-stranded DNA (ssDNA) probe.**

To demonstrate the exceptional sensitivity of our PWSPR biosensor system towards miR-21, we conducted a series of tests. Initially, a PBS solution was injected into the reaction chamber using a peristaltic pump at a flow rate of 20uL/min for 35 minutes to establish a long-term background noise profile. Following this, a solution containing 50pM miR-21 was introduced under identical conditions and allowed to undergo a 30-minute hybridization reaction. After this, the chamber was washed with PBS at a flow rate of 200uL/min for 5 minutes, and then PBS was reintroduced to measure the post-reaction response. Figure 4(a) illustrates the time response of the DNA/RNA hybridization compared to the background noise, revealing a significant distinction between the ultra-low concentration of 50pM miR-21 and the background noise. Figure 4(b) shows a bar graph of the magnitude response data from both test conditions, highlighting the difference in response before and after the 30-minute hybridization period. In this figure, the values for the magnitude response of 50pM miRNA ( $R_{mi}$ ) and the blank ( $R_{blank}$ ) were derived using formula (1). These graphs clearly differentiate the hybridization response of 50pM miR-21, showing values more than six times higher than the background noise without any overlap in error bars. Based on these foundational measurements, it's determined that this system can detect miR-21 at limits as low as 50pM.

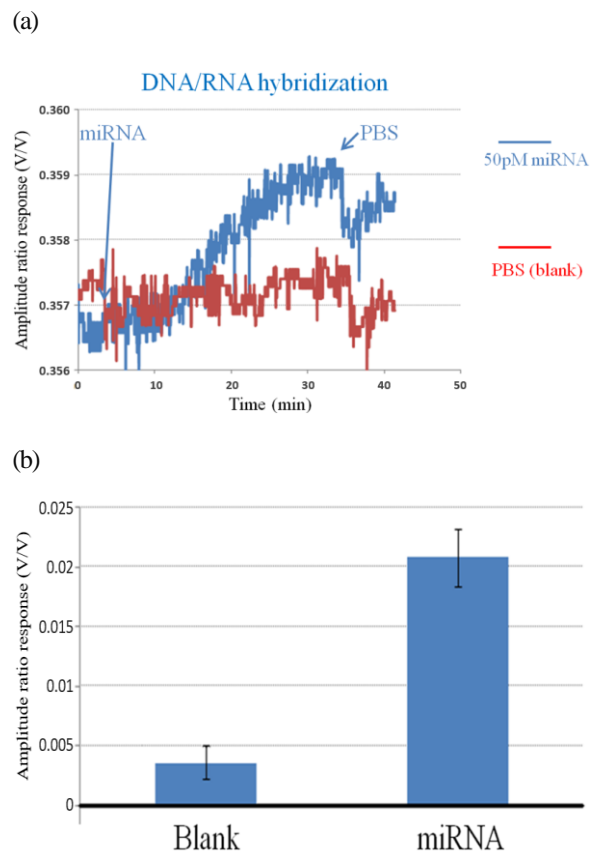


**Figure 4. (a) This graph shows how the binding strength between 50 pM miR-21 and its perfectly-matched DNA probe changes over time, illustrating the dynamic response of their interaction. (b) Here, we compare the hybridization results of the miR-21 probe with a blank sample, highlighting the differences in their hybridization behaviors.**

In exploring miRNA, we focus on the quantitative hybridization kinetics between DNA probes and miR-21 in solution. To calculate the affinity constant ( $K_A$ ), we employ the simple Langmuir isotherm [equation (2)], utilizing OriginPro software for nonlinear curve fitting. Figure 5 presents the Langmuir isotherm for miR-21/DNA hybridization across various miRNA concentrations (1, 5, 10, 50, 200, 500, and 1000nM). From this analysis, we've deduced a  $K_A$  value of  $3.7 \times 10^8 M^{-1}$  through linear regression for targets that are fully complementary. This finding indicates a slightly higher affinity constant for this test compared to the 16mer DNA hybridization at a 50nM concentration, which had a value of  $2.0 \times 10^7 M^{-1}$ . [Ref] Clearly, this method, supported by the precision of OriginPro for curve fitting, proves effective for detecting miR-21 targets at a concentration of 50nM, showcasing its suitability for precise miRNA analysis. This indicates that the initial rate of reaction is connected to the fractional surface coverage of DNA-RNA heteroduplexes, as described by the Langmuir isotherm. This relationship can serve as a reliable indicator of the target microRNA (miRNA) concentration, offering a practical method for

quantifying specific nucleic acid interactions in a given sample.

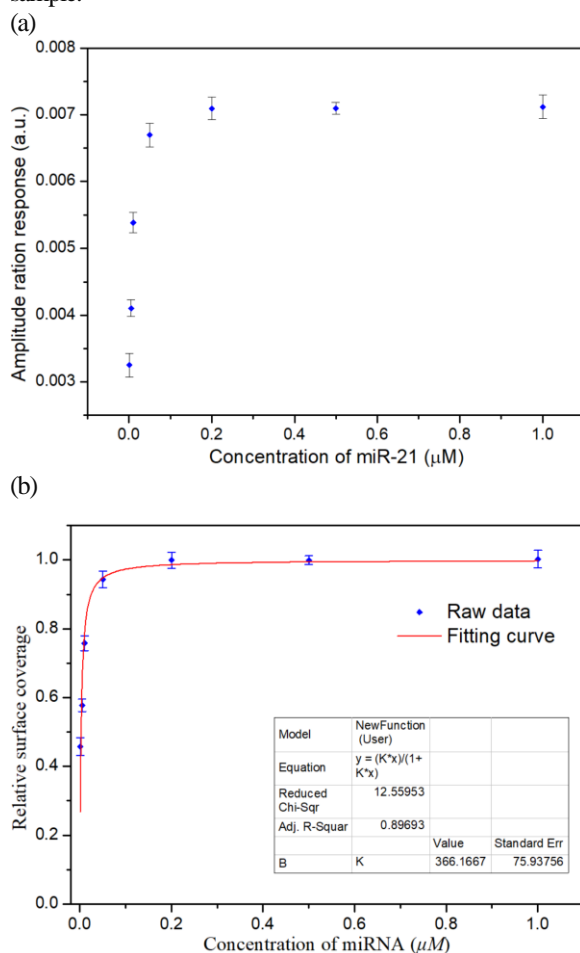


**Figure 5. (a) The amplitude responses of the binding of a perfectly matched miR-21 for deducing the affinity constant,  $K_A$ . The concentrations of miR-21 were explored at 1, 5, 10, 50, 200, 500 and 1000nM. The R-square from 1 to 1000nM is 0.897. (b) The fitting curve of Langmuir isotherm using OriginPro software to illustrate the relationship of DNA/RNA hybridization.**

## VI. CONCLUSIONS

In our research, we introduced a dual-channel PWSPR optical platform designed specifically for the detection of unlabeled oligonucleotides, thereby eliminating the necessity for any steps following hybridization. Through the addition of the dual-channel configuration and the optical heterodyne techniques, we've significantly reduced environmental noise, paving the way for real-time, highly sensitive biosensing applications. The capability of our system to detect 21-mer miR-21 at picomolar levels (as low as 50 pM) highlights the high sensitivity of our dual-channel PWSPR method in enhancing SPR signal detection. Our research further demonstrates that the integration of dual-channel setups with PWSPR measurements, combined with a straightforward application of the Langmuir

adsorption isotherm, yields an affinity constant ( $K_A$ ) of  $3.7 \times 10^8 \text{ M}^{-1}$  for DNA/miR-21 interactions at the biosensor surface. This finding indicates our system's potential to detect even shorter nucleotide sequences, positioning it as a valuable asset for miR-21 detection and wider biomedical research. Importantly, our method facilitates specific miRNA detection without the need for PCR amplification or any additional sample processing, simplifying miRNA analysis. Although our experiments were conducted on gold thin films, our system's adaptability to other substrates, such as glass or silicon, and its compatibility with a variety of detection methods, including electrochemical assays and fluorescence labeling, underscore its versatility. We are optimistic that our contributions will lead to the development of innovative biosensors that merge surface enzymatic activities with multiplexed bioaffinity interactions, setting new standards for specificity and sensitivity in the field.

## ACKNOWLEDGMENTS

This study was partially supported by the National Science Council of Taiwan (NSC98-2221-E-182-063-MY3, NSC98-2221-E-182-064-MY3), and Healthy Aging Research Center (HARC) in Chang Gung University. The support from the Ministry of Education, aiming from the Top University Plan (EMRPD 1A0751) is also appreciated.

## REFERENCES

- [1] C.-W. Tung, P.-Y. Huang, S. C. Chan, P.-H. Cheng and S.-H. Yang, "The regulatory roles of microRNAs toward pathogenesis and treatments in Huntington's disease," *Journal of Biomedical Science*, Vol. 132, no. 11, e159179,
- [2] T. Fehlmann, B. Lehallier, N. Schaum, O. Hahn, M. Kahraman, Y. Li, N. Grammes, L. Geffers, C. Backes, R. Balling, F. Kern, R. Krüger, F. Lammert, N. Ludwig, B. Meder, B. Fromm, W. Maetzler, D. Berg, K. Brockmann, C. Deuschle, A.-K. von Thaler, G. W. Eschweiler, S. Milman, N. Barzilai, M. Reichert, T. Wyss-Coray, E. Meese and A. Keller, "Common diseases alter the physiological age-related blood microRNA profile," *Nature Communications*, Vol. 11, 5958, Nov. 2020.
- [3] M. R. Kalthori, M. Soleimani, R. Alibakhshi, A. A. Kalthori, P. Mohamadi, R. Azreh and M. H. Farzaei, "The Potential of miR-21 in Stem Cell Differentiation and its Application in Tissue Engineering and Regenerative Medicine," *Stem Cell Reviews and Reports*, Vol. 19, pp. 1232–1251, Mar. 2023.
- [4] J. Rhim, W. Baek, Y. Seo and J. H. Kim, "From Molecular Mechanisms to Therapeutics: Understanding MicroRNA-21 in Cancer," *Cells*, Vol. 11, Iss. 18, 2791, Sep. 2022.
- [5] B. F. Far, K. Vakili, M. Fathi, S. Yaghoobpoor, M.

- Bhia c and M. R. Naimi-Jamal," The role of microRNA-21 (miR-21) in pathogenesis, diagnosis, and prognosis of gastrointestinal cancers: A review," *Life Sciences*, Vol. 316, 121340, Mar. 2023.
- [6] D. Bautista-Sánchez, C. Arriaga-Canon, A. Pedroza-Torres, I. A. D. L. Rosa-Velázquez, R. González-Barrios, L. Contreras-Espinosa, R. Montiel-Manríquez, C. Castro-Hernández, V. Fragosó-Ontiveros, R. M. Álvarez-Gómez and L. A. Herrera," The Promising Role of miR-21 as a Cancer Biomarker and Its Importance in RNA-Based Therapeutics" *Molecular Therapy Nucleic Acids*, Vol. 20, pp. 409-420, Jun. 2020.
- [7] B. Dai, F. Wang, X. Nie, H. Du, Y. Zhao, Z. Yin, H. Li, J. Fan, Z. Wen, D. W. Wang and C. Chen," The Cell Type-Specific Functions of miR-21 in Cardiovascular Diseases," *Frontiers in Genetics*, Vol. 11, 563166, Nov. 2020.
- [8] B. Lagerbauer and S. Engelhardt," MicroRNAs as therapeutic targets in cardiovascular disease," *The Journal of Clinical Investigation*, Vol. 132, Iss. 11, e159179, Jun. 2022.
- [9] C. GaoI, D. ZhaoI, J. WangI, P. LiuI and B. Xu," Clinical significance and correlation of microRNA-21 expression and the neutrophil-lymphocyte ratio in patients with acute myocardial infarction," *Clinics*, Vol. 74, e1237, Jul. 2019.
- [10] A. Touhami, "Biosensors and nanobiosensors: Design and applications," *Nanomedicine*. 1st ed. One Central Press; Cheshire, UK: 2014. pp. 374-403.
- [11] M. A. Morales and J. M. Halpern, "Guide to Selecting a Biorecognition Element for Biosensors," *Bioconjugate Chemistry*, Vol. 29, no. 10, pp.3231-3239, Sep. 2018.
- [12] Y. Chen, J. Liu, Z. Yang, J. S. Wilkinson and X. Zhou, "Optical biosensors based on refractometric sensing schemes: A review," *Biosensors and Bioelectronics*, Vol. 144, no.1, 111693, Nov. 2019.
- [13] Z. Zhong, M. Fritzsche, S. B Pieper, T. K Wood, K. L Lear, D. S Dandy and K. F Reardon," Fiber optic monoxygenase biosensor for toluene concentration measurement in aqueous samples," *Biosensors and Bioelectronics*, Vol. 26, Iss. 5, pp. 2407-2412, Jan. 2011.
- [14] S. H. S. Mandala, T.-J. Liu, C.-M. Chen, K.-K. Liu, M. Januar, Y.-F. Chang, C.-S. Lai, K.-H. Chang, K.-C. Liu," Enhanced Plasmonic Biosensor Utilizing Paired Antibody and Label-Free Fe<sub>3</sub>O<sub>4</sub> Nanoparticles for Highly Sensitive and Selective Detection of Parkinson's  $\alpha$ -Synuclein in Serum," *Biosensors*, Vol. 11, Iss. 10, 402, Oct. 2021.
- [15] S. Liu, Z. Zheng and X. Li, "Advances in pesticide biosensors: current status, challenges, and future perspectives," *Analytical and Bioanalytical Chemistry*, Vol. 405, pp. 63-90, Aug. 2012.
- [16] L. A. Vuillaume, J. Frija-Masson, M. Hadjiat, T. Riquier, M.-P. d'Ortho, P. L. Borgne, C. Goetz, P. L. Voss, A. Ougazzaden, J.-P. Salvestrini and T. Leichlé, "Biosensors for the Rapid Detection of Cardiovascular Biomarkers of Vital Interest: Needs, Analysis and Perspectives," *Journal of Personalized Medicine*, Vol. 12, Iss. 12, 1942, Nov. 2022.
- [17] C. A Wartchow, F. Podlaski, S. Li, K. Rowan, X. Zhang, D. Mark and K.-S. Huang, "Biosensor-based small molecule fragment screening with biolayer interferometry," *Journal of Computer-Aided Molecular Design*, Vol. 25, no.7, pp. 669-76, Jul. 2011.
- [18] Y.-F. Chang, C. Fu, Y.-T. Chen, A. F.-J. Jou, C.-C. Chen, C. Chou and J.-A. A. Ho," Use of liposomal amplifiers in total internal reflection fluorescence fiber-optic biosensors for protein detection," *Biosensors and Bioelectronics*, Vol. 77, pp. 1201-1207, Mar. 2016.
- [19] Y.-F. Chang, K.-C. Tsao, Y.-C. Liu, Y.-C. Chen, P.-C. Yu, Y.-C. Huang and C. Chou," Diagnosis of human metapneumovirus in patients hospitalized with acute lower respiratory tract infection using a metal-enhanced fluorescence technique," *Journal of virological methods*, Vol. 213, pp. 151-156, Mar. 2015.
- [20] Y.-C. Li, Y.-F. Chang, L.-C. Su and C. Chou, "Differential-Phase Surface Plasmon Resonance Biosensor," *Analytical Chemistry*, Vol. 80, pp. 5590-5595, May 2008.
- [21] Y.-F. Chang, R.-C. Chen, Y.-J. Lee, S.-C. Chao, L.-C. Su, Y.-C. Li and C. Chou, "Localized surface plasmon coupled fluorescence fiber-optic biosensor for alpha-fetoprotein detection in human serum," *Biosensors and Bioelectronics*, Vol. 24, pp. 1610-1614, Feb. 2009.
- [22] Y.-C. Li, C.-C. Chiou, J.-D. Luo, W.-J. Chen, L.-C. Sua, Y.-F. Chang, Y.-S. Chang, C.-S. Lai, C.-C. Lee and C. Chou, "Sensitive detection of unlabeled oligonucleotides using a paired surface plasma waves biosensor," *Biosensors and Bioelectronics*, Vol. 35, pp. 342-348, May 2012.
- [23] I. Székács, N. Kaszás, P. Gróf, K. Erdélyi, I. Szendrő, B. Mihalik, Á. Pataki, F. A. Antoni and E. Madarász," Optical Waveguide Lightmode Spectroscopic Techniques for Investigating Membrane-Bound Ion Channel Activities," *PLoS ONE*, Vol. 8, no. 12, e81398, Dec. 2013.
- [24] K. Majer-Baranyi, F. Szendrei, N. Adányi and A. Székács," Application of Highly Sensitive Immunosensor Based on Optical Waveguide Light-Mode Spectroscopy (OWLS) Technique for the Detection of the Herbicide Active Ingredient Glyphosate," *Biosensors*, Vol. 13, no. 8, 77, Jul. 2023.
- [25] A. Atapour, H. Khajehzadeh, M. Shafie, M. Abbasi, S. Mosleh-Shirazi, S. R. Kasaei and A. M. Amani," Gold nanoparticle-based aptasensors: A promising perspective for early-stage detection of cancer biomarkers," *Materials Today Communications*, Vol. 30, 103181, Mar. 2022.
- [26] S. H. S. Mandala, T.-J. Liu, C.-M. Chen, K.-K. Liu, M. Januar, Y.-F. Chang, C.-S. Lai, K.-H. Chang and

- K.-C. Liu," Enhanced Plasmonic Biosensor Utilizing Paired Antibody and Label-Free Fe<sub>3</sub>O<sub>4</sub> Nanoparticles for Highly Sensitive and Selective Detection of Parkinson's  $\alpha$ -Synuclein in Serum," *Biosensors*, Vol. 11, Iss. 10, 402, Oct. 2021.
- [27] J.J. Storhoff, S.S. Marla, P. Bao, S. Hagenow, H. Mehta, A. Lucas, V. Garimella, T. Patno, W. Buckingham, W. Cork and U. R. Müller, "Gold nanoparticle-based detection of genomic DNA targets on microarrays using a novel optical detection system," *Biosensors and Bioelectronics*, Vol. 19, pp. 875-883, Mar. 2004.
- [28] S. Sang, Y. Wang, Q. Feng, Y. Wei, J. Ji and W. Zhang, "Progress of new label-free techniques for biosensors: a review," *Critical Reviews in Biotechnology*, Vol. 36, no. 3, pp. 465-481, Jan. 2015.
- [29] Y. Wang, M. A. Ali, E. K. C. Chow, L. Dong and M. Lu, "An optofluidic metasurface for lateral flow-through detection of breast cancer biomarker," *Biosensors and Bioelectronics*, Vol. 107, no. 1, pp. 224-229, Jun. 2018.
- [30] E. Wijaya, C. Lenaerts, S. Maricot, J. Hastanin, S. Habraken, J.-P. Vilcot, R. Boukherroub and S. Szunerits, "Surface plasmon resonance-based biosensors: From the development of different SPR structures to novel surface functionalization strategies," *Current Opinion in Solid State and Materials Science*, Vol. 15, Iss. 5, pp. 208-224, Oct. 2011.
- [31] H. Raether, "Surface Plasmons on Smooth and Rough Surfaces and on Gratings," New York, Springer-Verlag: 118-119, 1988.
- [32] J. Homola, "Present and future of surface plasmon resonance biosensors," *Analytical and Bioanalytical Chemistry*, Vol. 377, pp. 528-539, July 2003.
- [33] E. Milkani, S. Morais, C. R. Lambert and W. G. McGimpsey, "Detection of oligonucleotide systematic mismatches with a surface plasmon resonance sensor," *Biosensors and Bioelectronics*, Vol. 25, Iss. 5, pp. 1217-1220, Jan. 2010.
- [34] M.-C. Li, Y.-F. Chang, H.-Y. Wang, Y.-X. Lin, C.-C. Kuo, J.-A. A. Ho, C.-C. Lee and L.-C. Su, "An innovative application of time-domain spectroscopy on localized surface plasmon resonance sensing," *Scientific Reports*, Vol. 7, 44555, Mar. 2017.
- [35] Y.-F. Chang, W.-H. Wang, Y.-W. Hong, R.-Y. Yuan, K.-H. Chen, Y.-W. Huang, P.-L. Lu, Y.-H. Chen, Y.-M. A. Chen, L.-C. Su and S.-F. Wang, "Simple Strategy for Rapid and Sensitive Detection of Avian Influenza A H<sub>7</sub>N<sub>9</sub> Virus Based on Intensity-Modulated SPR Biosensor and New Generated Antibody," *Analytical chemistry*, Vol. 90, Iss. 3, pp. 1861-1869, Jan. 2018.
- [36] L.-C. Su, Y.-C. Tian, Y.-F. Chang, C. Chou and C.-S. Lai, "Rapid detection of urinary polyomavirus BK by heterodyne-based surface plasmon resonance biosensor," *Journal of Biomedical Optics*, Vol. 19, Iss. 1, 011013, Sep. 2013.
- [37] H. Šípová, S. Zhang, A. M. Dudley, D. Galas, K. Wang and J. Homola, "Surface Plasmon Resonance Biosensor for Rapid Label-Free Detection of Microribonucleic Acid at Subfemtomole Level," *Analytical Chemistry*, Vol. 82, Iss. 24, pp. 10110-10115, Nov. 2010.
- [38] H. J. Lee, A. W. Wark and Robert M. Corn, "Creating Advanced Multifunctional Biosensors with Surface Enzymatic Transformations," *Langmuir*, Vol. 22, Iss. 12, pp. 5241-5250, Apr. 2006.
- [39] M. A. Islam, M. A. Chowdhury, M. S. I. Mozumder and M. T. Uddin, "Langmuir Adsorption Kinetics in Liquid Media: Interface Reaction Model," *ACS Omega*, Vol. 6, Iss. 22, pp. 14481-14492, May 2021.



**Ying-Chang Li** is an assistant professor in the Graduate Institute, Prospective Technology of Electrical Engineering and Computer Science of National Chinyi University of Technology, Taiwan. He has a Ph.D. degree in Optics and Photonics (2012). His research interests include optical measurement, semiconductor process and biomedical optoelectronics.



**Li-Chen Su** is an associate professor in the General Education Center of Ming Chi University of Technology, Taiwan. She has a Master degree (2007) and Ph.D. degree (2012) in Optics and Photonics. Her research interests include Physics and biomedical optoelectronics.



**Chuan-Chian Chiou** is a professor in Department of Medical Biotechnology and Laboratory Science of Chang Gung University, Taiwan. He has a Master degree (1992) and Ph.D. degree (1997) in Life Science. His research interests include nucleic acid chemistry, cell and molecular biology, reagent development.



**Chien Chou** is a professor in Graduate Institute of Electro-Optical Engineering Chang Gung University, Taiwan. He has a Master degree (1975) and Ph.D. degree (1978) in Biomedical Optics. His research interests include optical measurement, and biomedical optoelectronics.

